
UnCLE: Benchmarking Unsupervised Continual Learning for Depth Completion

Xien Chen, Rit Gangopadhyay, Michael Chu, Patrick Rim, Hyungseob Park, Alex Wong

Abstract

We propose UnCLE, the first standardized benchmark for Unsupervised Continual Learning of a multimodal 3D reconstruction task: Depth completion aims to infer a dense depth map from a pair of synchronized RGB image and sparse depth map. We benchmark depth completion models under the practical scenario of unsupervised learning over continuous streams of data. While unsupervised learning of depth boasts the possibility to continuously learn novel data distributions over time, existing methods are typically trained on a static, or stationary, dataset. However, when adapting to novel nonstationary distributions, they “catastrophically forget” previously learned information. UnCLE simulates these non-stationary distributions by adapting depth completion models to sequences of datasets containing diverse scenes captured from distinct domains using different visual and range sensors. We adopt representative methods from continual learning paradigms and translate them to enable unsupervised continual learning of depth completion. We benchmark these models across indoor and outdoor environments, and investigate the degree of catastrophic forgetting through standard quantitative metrics. We find that unsupervised continual learning of depth completion is an open problem, and we invite researchers to leverage UnCLE as a foundational development platform.

1 Introduction

Autonomous navigation, robotic manipulation, and augmented, virtual, and extended realities (AR/VR/XR) are some of the many applications that rely on a reconstruction of the three-dimensional (3D) environment or scene. These applications are deployed on systems with heterogeneous sensors. Amongst them, visual (e.g., RGB camera) and range (e.g., time-of-flight, lidar) sensors are vital for recovering a metric-scale reconstruction, in the form of an egocentric range or depth map, to support these spatial applications. Fusion of returns from these two sensors necessitates a multimodal model that takes synchronized calibrated RGB image and sparse point cloud (typically projected onto the image plane as a sparse depth map) as input to recover a dense depth map, i.e., depth completion.

Depth completion models can be trained in a supervised [1, 2, 3] or unsupervised manner [4, 5, 6]. The former relies on ground truth, which is prohibitively expensive to acquire; what is called “ground truth” is actually the result of offline data processing that involves aggregation of sequences of RGB images and sparse point clouds followed by manual annotation to clean up erroneous or ambiguous regions [7], which is not scalable. The latter relies on principles of Structure-from-Motion (SfM) [8, 9], which is realized as a joint optimization of depth and pose estimation by minimizing RGB image and sparse range reconstruction objectives. Without the need for human annotation, unsupervised depth completion models boast the potential to continually learn and adapt to new 3D environments from the virtually limitless amount of un-annotated data in a life-long fashion.

However, this potential is far from realized: existing depth completion models are predominately trained on a dataset under the assumption that the distribution of 3D scenes is stationary. When extended to a sequence of datasets, we find that as unsupervised depth completion models learn from or fit to new data, they inevitably “forget” previously learned information from past dataset(s). Due

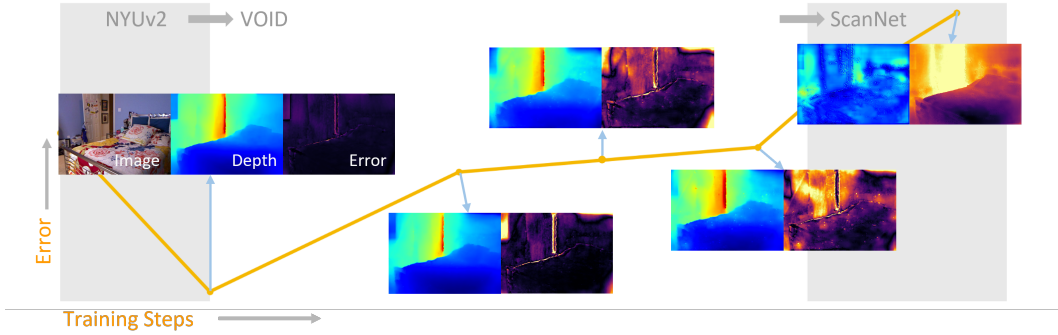


Figure 1: Error progression during continual unsupervised depth completion with a state-of-the-art continual learning method (ANCL). The model is initially on NYUv2, and continually trained on VOID and then ScanNet. Despite using a continual learning method, error increases over time, especially for later training steps.

to evolving conditions and unseen domains, the updates to the model parameters lead to significant performance degradation on previously learned datasets when fitting to new data distributions [10, 11, 12, 13]. This phenomenon is commonly referred to as “catastrophic forgetting.” Even when applying mitigation strategies, we observe an increase in error as training progresses, as shown in Fig. 1, which underscores the difficulty of addressing forgetting in unsupervised depth completion.

One school of thought is to re-train these models on the new data along with all previously collected datasets offline. This amounts to increasing computational costs that scale with the size of newly collected data. Additionally, due to initialization and stochasticity of optimization, the newly trained model may exhibit errors absent in the old one [14] – leading to performance regression. We, instead, subscribe to continual (or lifelong) learning, which is the training paradigm that addresses the challenge of catastrophic forgetting by enabling a single model to learn from a continuous stream of datasets, adapting to new datasets while preserving performance on previous ones. Therefore, we investigate unsupervised continual learning for depth completion, aiming to enable a multimodal depth estimation model to learn new datasets without forgetting, with the goal of fostering research that will culminate in models that can learn and adapt their inference without human intervention.

To this end, we propose a comprehensive benchmark for unsupervised continual learning of depth completion, termed “UnCLE”. We begin with the motivating observation of how the performance of three unsupervised depth completion models [4, 5, 15] degrades after being finetuned on sequences of datasets. We adopt five canonical continual learning methods (i.e., regularization-based [16, 17, 18] and rehearsal-based [19, 20] methods) and translate them for depth completion to mitigate catastrophic forgetting in this multimodal 3D reconstruction task. The benchmark evaluates methods on five dataset sequences, comprising six diverse datasets [4, 7, 21, 22, 23, 24] that were collected with different cameras and range sensors (see Fig. 2). UnCLE presents transitions between indoor scenes, outdoor scenes, and across indoor and outdoor scenes, a challenging scenario that no method has demonstrated performance on before. Through extensive hyper-parameter search for all depth completion and continual learning methods across all sequences, amounting to over a thousand experiments, we conclude that unsupervised continual learning for depth completion remains an open problem. UnCLE aims to serve as the first benchmark to streamline further research in this area.

Our contributions are as follows: (i) We propose UnCLE, the first standardized benchmark for unsupervised depth completion. (ii) We adapt existing, canonical regularization-based and rehearsal-based continual learning methods for unsupervised depth completion, presenting the first continual unsupervised depth completion methods. (iii) We introduce novel evaluation metrics tailored to continual depth completion—Average Forgetting, Average Performance, and Stability-Plasticity Trade-Off—to allow for comprehensive assessment of method behavior. (iv) Through 1,000+ experiments, we show that even the state-of-the-art continual learning methods exhibit a high degree of forgetting and performance for the task of depth completion on this challenging benchmark.

2 Related Works

Regularization-based Continual Learning approaches introduce constraints to the loss function to ensure that model behavior learned from previous datasets is not significantly altered. Amongst these

methods, one research thread constrains changes to model parameters that are deemed important for previous datasets. Elastic Weight Consolidation (EWC) [16] selectively decreases the plasticity of model weights determined by the Fisher information matrix. [25] estimates parameter importance based on their contribution to loss changes during training. [26] assesses importance by measuring the sensitivity of model outputs to parameter variations. [27] combines [16] and [25] to leverage their strengths. Another thread focuses on function regularization, which aims to preserve model output behavior on previous datasets by constraining changes in intermediate features or final predictions through knowledge distillation (KD) [28]. Learning without Forgetting (LwF) [17] leverages new data samples to approximate the responses of the old model. LwM [29] integrates attention maps into the KD process to capture essential features, while EBLL [30] preserves feature reconstructions by utilizing dataset-specific autoencoders. GD [31] exploits external unlabeled data to extend regularization beyond the training set, while PODNet [32] and LUCIR [33] aim to preserve feature similarity. Bayesian approaches, such as FRCL [34] and FROMP [35], use probabilistic models to regularize the functional space. VCL [36] extends these ideas and uses variational inference to maintain a balance between stability and plasticity. More recently, ANCL [18] introduces an auxiliary network to mitigate forgetting through a learned regularizer. In this paper, we adopt EWC, LWF, and ANCL as they are milestone works of the regularization-based approaches.

Rehearsal-based Continual Learning approaches reintroduce previous observed examples during the training of new datasets. Experience Replay [19] uses a data ('replay') buffer to store actual samples from previous datasets to be trained on again to reinforce performance on previous datasets. Works along this thread propose data selection strategies for choosing the replay buffer, including randomized Reservoir Sampling [37, 38, 39], class-based sampling [40, 41]. Generative replay [42] utilizes GANs and VAEs to produce synthetic data mimicking previously observed data distributions. VAE-approaches [43, 44, 45, 46, 47, 48] are able to control the generated data labels, but suffer from blurry quality. GAN-approaches [48, 49, 50] improve the quality of the generated input data. Feature replay stores features instead of the raw data in order to reduce the storage burden. [51, 52, 53] use feature distillation between new and old models. [54] stores initial class statistics, like mean and covariance, to rectify biases in predictions. CMP [20] improves memory efficiency and long-term adaptability by combining meta-representation learning with an optimal buffer replay strategy that selects diverse and representative samples based on representation similarity. UnCLe adopts Experience Replay and CMP as representative rehearsal-based continual learning methods.

Continual Learning for Depth Estimation. MonoDepthCL [55] employs a dual-memory rehearsal-based method to address the challenges of catastrophic forgetting in unsupervised monocular depth estimation. CoDEPS [56] employs a unique domain-mixing strategy for pseudo-label generation with efficient experience replay. However, previous works in this field typically focus on a single modality and lack standardized benchmarks, limiting their applicability to real-world scenarios where the use of multimodal data is standard. Our paper contributes to this field by establishing a benchmark for depth completion using both RGB images and sparse range data, addressing these gaps and setting a foundation for future research in continual depth estimation.

Depth Completion [57, 58, 59, 60] is the task of inferring a dense metric depth from an RGB image and synchronized sparse point cloud. *Supervised methods* [1, 61, 62, 63, 64, 65, 66, 67] minimize discrepancy between model estimates and ground-truth dense depth maps. While effective, these approaches are limited by the availability and cost of obtaining ground truth, making them less practical for continual learning scenarios. *Unsupervised depth completion* methods [4, 6, 15, 57, 59, 68, 69, 70] are trained by minimizing a loss function comprising image and sparse depth reconstruction terms along with a local smoothness regularizer. [68] utilizes Perspective-n-Point [71] and RANSAC [72] to align adjacent video frames. [57] trains a depth prior conditioned on the image. FusionNet [15] leverages synthetic data to learn a prior on shapes, while [73] leverage sim2real adaptation to make use of rendered synthetic depth. VOICED [4] approximates a scene with scaffolding. [70] introduces an adaptive scheme to reduce penalties incurred on occluded regions. KBNNet [5] proposes calibrated back-projection. [6] decouples scale and structure. [74] uses visual SLAM features and [58] proposes monitored distillation for positive congruent training.

However, all of these methods are subject to catastrophic forgetting as they rely on updating model weights to fit onto a new target dataset without the objective of retaining past information. This aspect makes it challenging for them to adapt to a continual learning setting, which aims to maintain performance on both new and previously seen datasets. We adopt VOICED, FusionNet, and KBNNet and evaluate them over five representative continual learning methods.

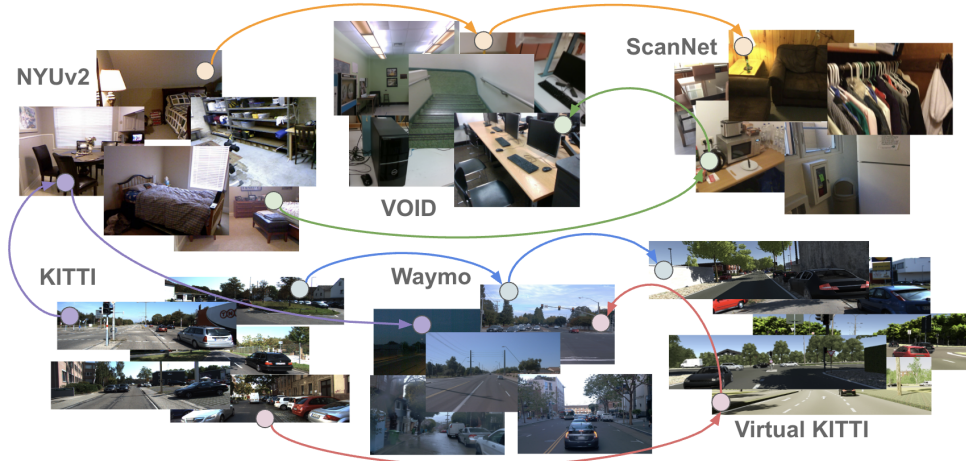


Figure 2: **Overview of benchmark.** UnCLE comprises six diverse datasets that are arranged into five sequences including indoor (orange, green arrows), outdoor (blue, red arrows), and indoor-outdoor (purple arrow). Each colored arrow path indicates a distinct dataset sequence used in our benchmark (e.g., NYUv2 → ScanNet → VOID for indoor, and KITTI → Waymo → Virtual KITTI for outdoor). Methods are evaluated on Average Forgetting, Average Performance, and Stability-Plasticity Trade-Off over four standard performance metrics.

3 Method Formulation

Problem definition. Unsupervised depth completion assumes a pair of synchronized RGB image and sparse depth map as input. Two time-adjacent RGB images are also assumed to be available during training. Let $I : \Omega \subset \mathbb{R}^2 \rightarrow \mathbb{R}_+^3$ denote an RGB image at current timestamp t obtained from a calibrated camera, and $z : \Omega \rightarrow \mathbb{R}_+$ the corresponding sparse depth map derived from a projected 3D point cloud. Given the image I , the sparse depth map z , and the intrinsic calibration matrix $K \in \mathbb{R}^{3 \times 3}$, the goal is to learn a function $\hat{d} = f_\theta(I, z)$ that estimates a dense depth map. Unsupervised methods are trained by minimizing photometric reprojection error between the observed image I_t and a reconstructed image \hat{I}_t from adjacent frames I_τ for $\tau \in \{t-1, t+1\}$ using the estimated depth \hat{d} and relative camera pose $g_{\tau t} \in SE(3)$:

$$\hat{I}_t(x, \hat{d}, g_{\tau t}) = I_\tau(\pi g_{\tau t} K^{-1} \bar{x} \hat{d}(x)). \quad (1)$$

where π denotes canonical perspective projection and \bar{x} the homogeneous coordinates $[x^\top, 1]^\top$ of $x \in \Omega$. $g_{\tau t}$ is given or estimated by a pose network and is only used during training.

In the continual learning setting, our objective is to adapt a pretrained model f_θ , trained on an initial dataset $D_0 = \{(I_0^{(i)}, z_0^{(i)}, K_0^{(i)})\}_{i=1}^{n_0}$, to a sequence of new datasets D_1, D_2, \dots, D_N , where each $D_k = \{(I_k^{(i)}, z_k^{(i)}, K_k^{(i)})\}_{i=1}^{n_k}$ and n_k denotes the number of training examples in T_k . The challenge is to incrementally train f_θ on each new target dataset D_k without experiencing significant degradation in performance on the source dataset S and all previously seen target datasets $D_j \forall j < k$. This requires effectively mitigating catastrophic forgetting while enabling the model to adapt across different domains or datasets in the depth completion task.

Unsupervised Depth Completion Loss. We train $f_\theta(I, z)$ by minimizing

$$\mathcal{L} = w_{ph} \ell_{ph} + w_{sz} \ell_{sz} + w_{sm} \ell_{sm} \quad (2)$$

where each loss term can be weighted by their respective w (see Sup. Mat. for details). The photometric consistency loss,

$$\ell_{ph} = \frac{1}{|\Omega|} \sum_{\tau \in T} \sum_{x \in \Omega} \left[w_{co} \left| \hat{I}_\tau(x) - I(x) \right| + w_{st} \left(1 - \text{SSIM}(\hat{I}_\tau(x), I(x)) \right) \right] \quad (3)$$

penalizes structural and color discrepancies between the reconstructed and observed images. The sparse depth consistency loss,

$$\ell_{sz} = \frac{1}{|\Omega|} \sum_{x \in \Omega} M(x) |\hat{d}(x) - z(x)| \quad (4)$$

Table 1: **Results on indoor.** Models are trained on NYUv2 and continually trained on ScanNet, then VOID.

Model	Method	Average Forgetting (%)				Average Performance (mm)				SPTO (mm)			
		MAE	RMSE	iMAE	iRMSE	MAE	RMSE	iMAE	iRMSE	MAE	RMSE	iMAE	iRMSE
VOICED	Finetuned	8.828	6.131	6.951	7.042	63.352	125.28	15.461	35.053	52.453	108.434	15.360	35.357
	EWC	9.439	8.014	5.183	6.174	63.787	126.706	15.229	34.367	53.614	110.956	15.091	34.039
	LwF	8.591	8.456	9.613	21.774	65.135	126.968	16.221	38.002	53.517	108.845	15.402	34.729
	Replay	6.154	4.688	9.471	11.713	64.305	126.714	16.373	36.729	54.326	112.218	16.640	37.671
	ANCL	6.796	5.870	6.206	14.586	86.653	134.761	167.249	203.559	80.039	139.843	91.895	121.101
	CMP	-0.365	-1.276	0.290	1.766	62.031	124.581	16.212	36.782	52.510	110.754	16.435	37.899
FusionNet	Finetuned	24.928	9.775	32.333	16.799	66.523	130.142	15.829	33.881	54.252	110.666	15.317	33.726
	EWC	11.256	8.782	17.944	17.847	64.487	130.890	15.264	34.203	51.345	109.223	14.276	32.781
	LwF	6.863	2.865	7.336	1.939	61.204	123.573	14.075	30.879	50.159	106.386	13.879	31.608
	Replay	5.702	2.862	12.196	11.186	61.467	125.587	14.750	33.279	50.273	108.608	14.351	33.658
	ANCL	3.952	5.392	8.765	16.647	68.963	141.313	18.380	42.584	57.390	122.924	18.044	41.724
	CMP	2.516	3.242	4.208	6.653	69.633	140.176	18.303	40.839	57.642	122.026	18.234	41.605
KBNet	Finetuned	16.080	15.463	8.188	9.170	58.577	124.606	13.474	31.409	47.890	105.807	13.266	31.742
	EWC	14.915	11.878	10.398	5.640	57.414	122.075	13.741	31.552	48.031	106.661	14.129	33.096
	LwF	9.717	6.324	6.168	5.254	57.511	119.093	14.119	32.165	47.154	103.164	14.304	33.838
	Replay	7.200	4.819	9.202	9.539	56.208	117.848	13.983	32.341	46.700	103.631	13.844	33.326
	ANCL	9.73	10.75	5.58	16.38	56.89	120.30	13.77	31.85	47.32	103.42	13.88	32.76
	CMP	5.39	5.11	8.25	7.90	55.92	117.83	13.74	31.43	46.03	102.36	13.55	32.03

grounds the predicted depth to metric scale, where $M : \Omega \subset \mathbb{R}^2 \rightarrow \{0, 1\}$ yields a binary mask of all valid sparse depth points. The local smoothness loss,

$$\ell_{sm} = \frac{1}{|\Omega|} \sum_{x \in \Omega} \lambda_X(x) |\partial_X \hat{d}(x)| + \lambda_Y(x) |\partial_Y \hat{d}(x)| \quad (5)$$

encourages smooth transitions of depth gradients in the x - (∂_X) and y - (∂_Y) directions, and is weighted by image gradients $\lambda_X = e^{-|\partial_X I_t(x)|}$ and $\lambda_Y = e^{-|\partial_Y I_t(x)|}$ to account for object edges.

3.1 Elastic Weight Consolidation

For the task of continual depth completion, we implement EWC as follows: When training on a new dataset T_k , we first load the previously trained model f_{θ^*} , which is parameterized by the weight matrices θ^* optimized for T_{k-1} . These parameters are frozen and treated as a reference during training on T_k . The Fisher information matrix F_i quantifies each parameter’s θ_i importance to the previous model’s performance on T_{k-1} . The EWC loss is therefore defined as:

$$\mathcal{L}_{ewc} = \lambda_{ewc} \sum_i \frac{1}{2} F_i (\theta_i - \theta_i^*)^2 \quad (6)$$

EWC loss penalizes important weights from moving too far away from their values optimized for the previous dataset. We add \mathcal{L}_{ewc} to the unsupervised loss \mathcal{L} (Eq. 2) with $\lambda_{ewc} = 1$, which we found to be optimal after extensive tuning, when choosing EWC as the continual learning method.

3.2 Learning without Forgetting

To implement Learning without Forgetting (LwF) for the depth completion datasets, we aim to preserve output behavior from previous tasks while training only on new data. Specifically, we load the checkpoint of the old model f_{θ^*} , which is kept frozen during training. We compute a mean squared error (MSE) loss between the outputs of the frozen model and the new model f_{θ} . The LwF loss encourages the new model’s predictions to remain consistent with that of the frozen model:

$$\mathcal{L}_{lwf} = \lambda_{lwf} \cdot \|f_{\theta}(I, z) - f_{\theta^*}(I, z)\|_2^2 \quad (7)$$

where $\lambda_{lwf} = 0.5$ is empirically determined. We add \mathcal{L}_{lwf} to \mathcal{L} (Eq. 2) when choosing LwF as the continual learning method. LwF allows the model to learn from new depth data without requiring access to previous task data, as the frozen model’s predictions act as a proxy for past knowledge.

3.3 Experience Replay

To perform experience replay with depth completion, we maintain a replay buffer, which retains a fixed number of representative samples from each dataset previously trained on. The selections and

Table 2: **Results on indoor.** Models are trained on NYUv2 and continually trained on VOID, then ScanNet.

Model	Method	Average Forgetting (%)				Average Performance (mm)				SPTO (mm)			
		MAE	RMSE	iMAE	iRMSE	MAE	RMSE	iMAE	iRMSE	MAE	RMSE	iMAE	iRMSE
VOICED	Finetuned	3.066	2.475	4.815	5.571	64.946	130.229	17.842	39.909	51.581	107.829	15.904	36.604
	EWC	3.189	1.893	6.874	8.376	64.850	129.705	17.955	40.526	51.639	108.317	16.055	37.330
	LwF	8.058	5.496	11.476	11.741	68.079	133.513	20.004	43.943	53.951	109.904	17.853	39.579
	Replay	7.588	4.717	19.605	20.487	71.119	139.216	21.754	46.938	57.968	116.636	19.699	42.695
	ANCL	14.200	7.096	20.185	16.408	71.180	135.583	19.998	43.718	53.742	112.189	17.618	40.213
	CMP	6.923	4.259	14.240	18.545	66.639	132.781	19.699	44.404	55.596	115.432	18.129	41.823
FusionNet	Finetuned	-0.932	1.872	-3.863	-0.875	65.716	134.609	17.112	38.915	51.246	110.127	14.919	35.577
	EWC	2.966	4.946	4.077	9.404	67.140	136.901	17.897	40.665	52.654	112.293	15.734	37.287
	LwF	-5.189	-4.175	-12.703	-13.945	63.697	128.577	16.005	35.141	49.659	104.974	13.894	32.027
	Replay	-0.042	0.021	-0.575	-1.335	66.128	134.107	17.877	39.781	51.885	110.235	15.498	35.965
	ANCL	10.818	9.102	16.138	21.646	74.731	149.734	21.780	48.898	60.476	127.344	19.485	45.069
	CMP	13.970	10.112	24.404	29.053	75.401	149.310	22.792	51.279	61.368	127.004	20.395	47.038
KBNet	Finetuned	16.111	17.678	9.807	13.391	63.064	134.674	15.650	36.275	44.986	101.266	12.971	31.393
	EWC	10.516	13.401	5.126	8.996	61.393	131.994	15.823	36.532	45.951	103.006	13.530	32.465
	LwF	11.110	6.110	12.480	13.539	61.797	126.955	17.367	39.599	46.784	102.881	14.750	34.807
	Replay	7.501	5.230	9.862	10.223	58.972	125.088	16.435	37.717	46.711	103.417	14.326	34.077
	ANCL	6.799	4.797	8.117	8.647	61.915	131.275	17.487	39.455	49.083	110.329	15.733	37.085
	CMP	14.005	9.561	24.587	29.524	64.330	135.738	19.138	44.763	51.741	115.460	17.089	41.576

Table 3: **Results on outdoors.** Models are trained on KITTI and continually trained on Waymo, then VKITTI.

Model	Method	Average Forgetting (%)				Average Performance (mm)				SPTO (mm)			
		MAE	RMSE	iMAE	iRMSE	MAE	RMSE	iMAE	iRMSE	MAE	RMSE	iMAE	iRMSE
VOICED	Finetuned	499.598	162.188	467.472	208.693	1620.429	3072.129	4.040	6.144	914.223	2993.228	1.955	4.503
	EWC	555.925	190.152	540.109	247.943	1796.300	3346.057	4.490	6.685	962.937	3209.759	1.962	4.739
	LwF	631.119	221.535	524.976	233.758	1973.972	3612.700	4.533	6.648	985.995	3236.244	2.062	4.722
	Replay	17.241	4.050	16.662	5.478	524.114	1875.897	1.333	3.359	618.668	2366.577	1.292	3.348
	ANCL	178.694	64.382	170.133	80.818	1019.338	2317.409	2.392	4.425	881.934	2641.127	1.790	3.965
	CMP	37.689	14.711	70.463	50.115	1451.306	3226.971	2.319	4.396	1491.603	3686.281	2.081	4.200
FusionNet	Finetuned	11.336	8.435	17.447	17.991	437.730	1785.212	1.193	3.724	501.362	2138.422	1.111	3.978
	EWC	21.006	10.494	20.431	16.535	431.440	1760.460	1.144	3.181	486.170	2117.030	1.029	2.986
	LwF	12.368	5.202	13.593	13.117	442.878	1759.202	1.178	3.352	526.528	2168.961	1.156	3.451
	Replay	8.290	11.134	2.769	7.975	419.044	1774.361	1.044	3.032	479.168	2122.997	0.966	2.906
	ANCL	6.717	7.089	6.164	10.803	404.664	1716.474	1.071	3.159	459.187	2055.770	0.988	3.065
	CMP	5.585	8.860	1.383	7.466	405.654	1743.608	1.042	3.073	462.593	2087.346	0.968	2.969
KBNet	Finetuned	27.153	18.208	52.969	33.370	469.658	1943.259	1.338	3.683	541.383	2411.169	1.144	3.505
	EWC	23.517	8.583	30.077	18.991	456.828	1806.761	1.221	3.321	526.366	2210.424	1.133	3.158
	LwF	21.184	4.049	43.500	19.951	460.097	1749.734	1.362	3.555	541.932	2142.999	1.359	3.731
	Replay	25.423	29.303	6.362	7.274	454.896	1935.667	1.102	3.203	525.696	2318.363	1.094	3.246
	ANCL	20.49	8.94	23.11	27.73	438.05	1795.76	1.21	3.56	503.53	2203.44	1.18	3.53
	CMP	15.95	15.47	6.90	7.39	507.90	2262.46	1.06	3.21	447.09	1887.14	1.09	3.19

the integration of the replay buffer into the new task are designed to balance computational efficiency with performance retention. Empirically, a buffer size of 64 data points for each previous dataset was determined to offer an optimal balance. During each training iteration on a new target dataset, a batch of data from the replay buffer is reintroduced into the training process. The data points from both the current and historical datasets are processed as follows:

Let $D_{\text{new}} = D_k$ denote the set of new training data points from the current target dataset, where N is the number of new data points. Similarly, let $D_{\text{replay}} = \{(I_r^{(j)}, z_r^{(j)}, K_r^{(j)})\}_{j=1}^M$ denote the set of replayed data points from the buffer, where M is the number of data points in the replay buffer. Each training batch is made up of a 50-50 new-replay data ratio, where the replay half is evenly split between previous datasets. The total loss function $\mathcal{L}_{\text{total}}$ for a training iteration is then formulated as:

$$\mathcal{L}_{\text{total}} = \mathcal{L}_{\text{new}} + \mathcal{L}_{\text{replay}} \quad (8)$$

where \mathcal{L}_{new} is the unsupervised loss \mathcal{L} in Eq. 2 computed on the new training data, and $\mathcal{L}_{\text{replay}}$ is the unsupervised loss \mathcal{L} computed on the replayed data.

3.3.1 Optimal Memory Buffer Retention Strategy

As a more recent replay-based method, we implemented the strategy from the CMP [20] method to more carefully select which samples to store in the replay buffer. Instead of randomly choosing a set

Table 4: **Results on outdoor.** Models are trained on KITTI and continually trained on VKITTI, then Waymo.

Model	Method	Average Forgetting (%)				Average Performance (mm)				SPTO (mm)			
		MAE	RMSE	iMAE	iRMSE	MAE	RMSE	iMAE	iRMSE	MAE	RMSE	iMAE	iRMSE
VOICED	Finetuned	474.009	165.136	370.424	155.125	2060.582	4376.605	3.562	6.024	1025.089	3418.751	2.040	4.630
	EWC	461.303	147.778	364.455	135.980	1750.973	3812.288	3.325	5.560	965.069	3216.165	1.968	4.434
	LwF	337.637	104.948	273.390	107.768	1494.371	3476.494	2.871	5.185	942.391	3125.526	1.923	4.296
	Replay	13.913	11.382	27.166	8.929	584.114	2329.848	1.304	3.274	615.781	2396.354	1.263	3.075
	ANCL	159.673	50.002	197.543	81.902	1113.680	2997.533	2.347	4.725	877.832	2869.267	1.799	4.107
	CMP	48.249	11.697	4.621	4.479	1070.327	2700.213	1.616	3.672	1440.935	3237.217	1.949	3.785
FusionNet	Finetuned	16.344	10.358	27.541	17.882	470.609	2082.091	1.093	3.355	510.531	2161.420	1.092	3.161
	EWC	12.313	9.516	35.145	23.740	459.507	93.598	1.082	3.367	493.153	2109.876	1.077	3.164
	LwF	1.651	-13.290	37.645	7.821	436.941	1932.231	1.090	3.347	496.067	2239.943	1.042	3.379
	Replay	6.715	9.282	6.068	7.796	436.402	2023.981	0.956	3.057	469.038	2082.781	0.966	2.907
	ANCL	6.814	7.446	11.704	13.729	435.777	2007.397	1.019	3.225	466.817	2069.395	1.019	3.038
	CMP	9.658	10.924	6.204	8.565	437.079	2030.872	0.988	3.186	466.370	2088.647	0.987	3.028
KBNet	Finetuned	19.842	11.959	17.144	14.162	469.095	2076.653	1.185	3.513	496.070	2140.853	1.155	3.299
	EWC	18.438	14.418	32.407	20.567	471.227	2131.648	1.141	3.476	501.447	2191.964	1.132	3.285
	LwF	14.797	4.244	68.109	33.271	496.194	2076.227	1.476	4.028	535.322	2170.847	1.415	3.830
	Replay	13.929	17.453	7.582	6.629	458.919	2156.319	1.023	3.279	491.371	2216.334	1.038	3.147
	ANCL	14.748	9.927	22.279	15.974	473.733	2151.693	1.062	3.419	505.116	2225.249	1.068	3.251
	CMP	15.170	15.887	9.719	7.491	463.297	2158.487	1.023	3.297	497.619	2229.364	1.036	3.166

Table 5: *Error metrics.* There are N datasets and k denotes the index of the most recently trained dataset D_k . Each a_j^k represents any of our depth completion metrics on dataset D_j after training on dataset D_k .

Metric	Definition
Average Forgetting (\bar{F})	$\frac{2}{N(N-1)} \sum_{k=1}^N \sum_{j < k} \frac{a_j^k - a_j^j}{a_j^j}$
Average Performance ($\bar{\mu}$)	$\frac{2}{N(N+1)} \sum_{k=1}^N \sum_{j \leq k} a_j^k$
Stability-Plasticity Trade-off (SPTO)	$\frac{2 \times S \times P}{S+P}, \begin{cases} S = \sum_{k=1}^N a_k^N \\ P = \sum_{k=1}^N a_k^k \end{cases}$

of samples from the previous datasets to store in the replay buffer, we attempt to store samples that show a similarity below some threshold δ . We do this by iterating through the dataset we want to replay in the next continual step D_{new} , and comparing the similarity of the next batch in this dataset $D_{new}^{(b)}$ and a randomly sampled batch that is already stored in the replay buffer $D_{replay}^{(b)}$ after being passed through a representation encoder f_θ . Thus, at each step of the iteration, we append $D_{new}^{(b)}$ to D_{replay} if similarity between $f_\theta(D_{new}^{(b)})$ and $f_\theta(D_{replay}^{(b)})$ is less than δ .

3.4 Auxiliary Network Continual Learning

Auxiliary Network Continual Learning (ANCL) introduces an auxiliary model to promote plasticity, complementing the main model’s focus on stability. For continual depth completion, we implement ANCL by maintaining two networks: the main model f_θ , and an auxiliary network $f_{\theta_{aux}}$, both initialized from the previously trained model on dataset D_{k-1} .

When training on a new dataset D_k , both the frozen parameters θ^* (from previous dataset) and the auxiliary model parameters θ_{aux} are used to compute constraints based on stability and plasticity. Specifically, the ANCL loss is a weighted sum of two Elastic Weight Consolidation (EWC) losses:

$$\mathcal{L}_{ancl} = \lambda_{ewc} \sum_i \frac{1}{2} F_i (\theta_i - \theta_i^*)^2 + \lambda_{aux} \sum_i \frac{1}{2} F_i (\theta_i - \theta_{aux,i})^2 \quad (9)$$

Here, the Fisher information matrix F_i is estimated for both the main and auxiliary models during continual training. To train the auxiliary model, we compute an unsupervised loss (Eq. 2) independently using the same inputs, and backpropagate this loss through $f_{\theta_{aux}}$ using a separate optimizer. We set $\lambda_{ewc} = 1.0$ and $\lambda_{aux} = 0.5$ based on validation performance. Fisher matrices for both networks are accumulated across epochs and updated after training on each dataset, consistent with EWC.

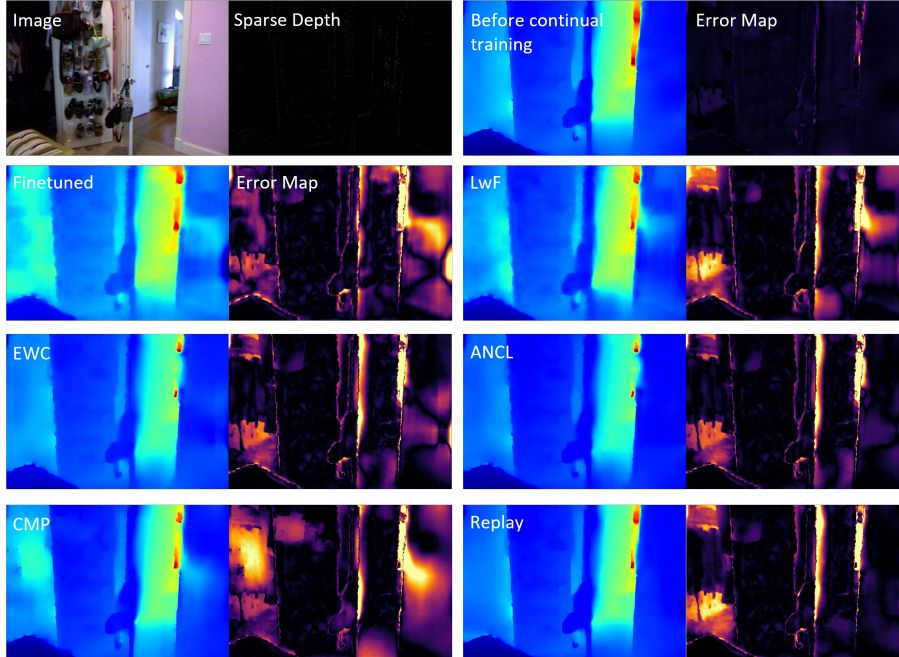


Figure 3: **Comparison on NYUv2 after continual training on VOID.** Rows 2-4 show results from models that were first trained on NYUv2 and then continually trained on VOID using different continual learning methods.

4 Experiments

For evaluation, we compute four metrics: Average Forgetting, Average Performance, and STPO on Mean Absolute Error (MAE), Root Mean Squared Error (RMSE), Inverse MAE (iMAE), and Inverse RMSE (iRMSE). Average Forgetting measures how much performance on previously learned datasets deteriorates after learning new ones. Average Performance reflects the overall accuracy across all seen datasets. Stability-Plasticity Trade-off (SPTO) quantifies the balance between preserving prior knowledge (stability) and acquiring new knowledge (plasticity) using a harmonic mean of final and intermediate performance. These metrics are computed over *all datasets*. See Table 5 for details.

Datasets. We use three datasets for indoor experiments and three datasets for outdoor experiments.

Indoor datasets: The **NYUv2** dataset [21] contains 464 indoor scenes captured using RGB-D sensors, offering 1449 densely labeled pairs of aligned RGB and depth images. It is a benchmark dataset widely used in indoor depth estimation tasks. NYUv2 is the primary dataset on which we pretrain our depth completion models before outdoor continual learning. The **VOID** dataset [4] provides sparse depth maps and RGB frames for indoor environments, with approximately 58,000 frames. VOID emphasizes handling low-texture regions and scenes with significant camera motion, which are crucial for testing robustness in indoor depth completion. **ScanNet** [22] is a large-scale indoor dataset that includes more than 2.5 million frames with corresponding RGB-D data. It provides dense depth ground truth and 3D reconstructions of indoor environments. We use the evaluation protocol in [4] and cap the evaluation range from 0.2 to 5 meters.

Outdoor datasets: The **KITTI** dataset [7] is a widely used benchmark for autonomous driving, consisting of over 93,000 stereo image pairs and sparse LiDAR depth maps synchronized with the images that were captured from a wider range of urban and rural scenes. KITTI is the primary dataset on which we pretrain our depth completion models before outdoor continual learning. The **Waymo** [23] Open Dataset includes approximately 230,000 frames of high-resolution images and dense LiDAR point clouds, covering a wide range of driving environments and conditions. **Virtual KITTI (VKITTI)**, [24] is a synthetic dataset designed to replicate KITTI scenes, providing over 21,000 frames with dense ground truth depth. It allows for evaluating domain adaptation, as we use multiple data domains to simulate domain discrepancies which cause catastrophic forgetting. For KITTI and VKITTI, we cap the evaluation range from 0.001 to 100 meters. For Waymo, we cap the evaluation range from 0.001 to 80 meters.

Protocol. For indoor sequences, we first train on NYUv2 and evaluate the continual learning process over sequences: NYUv2 \rightarrow ScanNet \rightarrow VOID (Table 1), and NYUv2 \rightarrow VOID \rightarrow ScanNet (Table 2). For outdoor sequences, we first train on KITTI and evaluate over sequences: KITTI \rightarrow Waymo \rightarrow Virtual KITTI (Table 3), and KITTI \rightarrow Virtual KITTI \rightarrow Waymo (Table 4). For the mixed-domain (indoor-outdoor) sequence, we first train on KITTI and evaluate the continual learning process over KITTI \rightarrow NYUv2 \rightarrow Waymo. Due to space constraints, the mixed experiments are positioned in the Supp. Mat. Figure 2 illustrates all datasets and the colored arrow paths corresponding to each of these training sequences used in our benchmark. All experiments were conducted using two servers, each equipped with 4 NVIDIA RTX 3090 GPUs (24GB VRAM per GPU).

4.1 Results

Quantitative. Due to space limitations, we defer raw results of MAE, RMSE, iMAE, and iRMSE across all datasets to the Supp. Mat. From Tables 1 and 2, we observe that for indoor continual learning, most methods outperform the finetuned baseline in terms of Average Forgetting across multiple models. In particular, **Replay** and **CMP** consistently outperform Finetuned in Table 1 across all metrics. **EWC** and **LwF** offer modest improvements over Finetuned in certain FusionNet and KNet rows, but are less reliable in VOICED. Surprisingly, the finetuning approach performs the worst in terms of Average Forgetting in *only 3 out of 6* scenarios (model-sequence pairing) for indoor datasets, and *4 out of 6* scenarios for outdoor datasets. In Average Performance, Finetuned only performs the worst in *3 out of 12* scenarios. This shows that when encountering complicated 3D tasks, existing continual learning methods are not guaranteed to improve performance.

For outdoor datasets (Tables 3 and 4), the performance gap between methods is larger. **Replay** reduces forgetting significantly compared to Finetuned in most rows, particularly in Table 3 for VOICED (17.241% vs. 499.598% forgetting). However, in Table 4, the forgetting advantage of Replay narrows, and **CMP** achieves comparable forgetting in FusionNet and KNet. **EWC** and **LwF** occasionally show worse forgetting than Finetuned outdoors, especially in VOICED, but achieve competitive SPTO in some FusionNet cases. **ANCL** performs stably in KNet and FusionNet, but loses to replay-based methods in VOICED. In addition, methods with the best Average Forgetting score do not always have the best Average Performance score. For example, in Table 3, CMP has the lowest Average Forgetting with KNet but is the worst in terms of Average Performance. These findings suggest that while replay-based methods often yield strong forgetting reduction, regularization-based methods ANCL can be competitive depending on the model and training sequence. Overall, *no single method dominates across all metrics and settings*, highlighting the importance of evaluating forgetting, learning, and trade-offs jointly in continual depth completion. This also leaves continual learning for depth completion tasks a challenging open question.

Qualitative. Fig. 3 shows that all continual learning methods develop artifacts in their predictions for the previously trained dataset, NYUv2 – even though they are only adapting to the first dataset of the sequence. When compared with the original pretrained model for NYUv2, they all perform poorly as they are not able to mitigate catastrophic forgetting. Additional examples are available in Supp. Mat.

5 Discussion

Limitations. The scope of our benchmark is restricted to existing canonical continual learning methods adapted to unsupervised depth completion; newer or task-specific methods remain unexplored. Also, we leave exploration of unsupervised continual learning for other tasks as future work.

Societal Impacts. Continual learning reduces the need to train separate models for new domains, lowering computational energy costs. It also promotes "backwards-compatibility" and positive-congruent models. However, it introduces the possibility for the model to forget safety-critical knowledge or learn unintended biases when exposed to uncurated or non-representative data.

To the best of our knowledge, this is the first study to apply continual learning methods to the problem of depth completion. By establishing a benchmark for continual depth completion across indoor and outdoor datasets, this paper sets the foundation for future work in extending continual learning to more complex, multimodal problems. We hope that this contribution will motivate further research into more effective strategies to combat catastrophic forgetting in depth completion and related 3D tasks. We invite the research community to join us in tackling this important open problem.

References

- [1] J. Park, K. Joo, Z. Hu, C. Liu, and I.-S. Kweon, “Non-local spatial propagation network for depth completion,” in *European Conference on Computer Vision (ECCV)*, 2020, pp. 120–136.
- [2] J. Kam, J. Kim, S. Kim, J. Park, and S. Lee, “Costdnet: Cost volume based depth completion for a single rgb-d image,” in *European Conference on Computer Vision*. Springer, 2022, pp. 257–274.
- [3] J. Tang, F.-P. Tian, B. An, J. Li, and P. Tan, “Bilateral propagation network for depth completion,” in *Proceedings of the IEEE/CVF Conference on Computer Vision and Pattern Recognition*, 2024, pp. 9763–9772.
- [4] A. Wong, X. Fei, S. Tsuei, and S. Soatto, “Unsupervised depth completion from visual inertial odometry,” *IEEE Robotics and Automation Letters*, vol. 5, no. 2, pp. 1899–1906, 2020.
- [5] A. Wong and S. Soatto, “Unsupervised depth completion with calibrated backprojection layers,” in *Proceedings of the IEEE/CVF International Conference on Computer Vision*, 2021, pp. 12 747–12 756.
- [6] Z. Yan, K. Wang, X. Li, Z. Zhang, J. Li, and J. Yang, “Desnet: Decomposed scale-consistent network for unsupervised depth completion,” in *Proceedings of the AAAI Conference on Artificial Intelligence*, ser. IEEE Robotics and Automation Letters, 2023, pp. 3109–3117.
- [7] A. Geiger, P. Lenz, and R. Urtasun, “Are we ready for autonomous driving? the kitti vision benchmark suite,” in *2012 IEEE Conference on Computer Vision and Pattern Recognition*. IEEE, 2012, pp. 3354–3361.
- [8] J.-M. Frahm, P. Fite-Georgel, D. Gallup, T. Johnson, R. Raguram, C. Wu, Y.-H. Jen, E. Dunn, B. Clipp, S. Lazebnik, *et al.*, “Building rome on a cloudless day,” in *Computer Vision—ECCV 2010: 11th European Conference on Computer Vision, Heraklion, Crete, Greece, September 5–11, 2010, Proceedings, Part IV 11*. Springer, 2010, pp. 368–381.
- [9] J. L. Schonberger and J.-M. Frahm, “Structure-from-motion revisited,” in *Proceedings of the IEEE conference on computer vision and pattern recognition*, 2016, pp. 4104–4113.
- [10] R. M. French, “Catastrophic forgetting in connectionist networks,” *Trends in cognitive sciences*, vol. 3, no. 4, pp. 128–135, 1999.
- [11] M. McCloskey and N. J. Cohen, “Catastrophic interference in connectionist networks: The sequential learning problem,” in *Psychology of learning and motivation*. Elsevier, 1989, vol. 24, pp. 109–165.
- [12] S. Thrun, “Is learning the n-th thing any easier than learning the first?” *Advances in neural information processing systems*, vol. 8, 1995.
- [13] R. Ratcliff, “Connectionist models of recognition memory: constraints imposed by learning and forgetting functions,” *Psychological review*, vol. 97, no. 2, p. 285, 1990.
- [14] S. Yan, Y. Xiong, K. Kundu, S. Yang, S. Deng, M. Wang, W. Xia, and S. Soatto, “Positive-congruent training: Towards regression-free model updates,” in *Proceedings of the IEEE/CVF Conference on Computer Vision and Pattern Recognition*, 2021, pp. 14 299–14 308.
- [15] A. Wong, S. Cicek, and S. Soatto, “Learning topology from synthetic data for unsupervised depth completion,” *IEEE Robotics and Automation Letters*, vol. 6, no. 2, pp. 1495–1502, 2021.
- [16] J. Kirkpatrick, R. Pascanu, N. Rabinowitz, J. Veness, G. Desjardins, *et al.*, “Overcoming catastrophic forgetting in neural networks,” *Proceedings of the national academy of sciences*, vol. 114, no. 13, pp. 3521–3526, 2017.
- [17] Z. Li and D. Hoiem, “Learning without forgetting,” in *Proceedings of the IEEE conference on computer vision and pattern recognition*, 2017, pp. 5077–5086.
- [18] S. Kim, L. Noci, A. Orvieto, and T. Hofmann, “Achieving a better stability-plasticity trade-off via auxiliary networks in continual learning,” in *Proceedings of the IEEE/CVF Conference on Computer Vision and Pattern Recognition (CVPR)*, 06 2023, pp. 11 930–11 939.
- [19] D. Rolnick, A. Ahuja, J. Schwarz, T. Lillicrap, and G. Wayne, “Experience replay for continual learning,” *Advances in neural information processing systems*, vol. 32, 2019.
- [20] D. Kang, D. Kum, and S. Kim, “Continual learning for motion prediction model via meta-representation learning and optimal memory buffer retention strategy,” in *Proceedings of the IEEE/CVF Conference on Computer Vision and Pattern Recognition*, 2024, pp. 15 438–15 448.
- [21] N. Silberman, D. Hoiem, P. Kohli, and R. Fergus, “Indoor segmentation and support inference from rgb-d images,” in *European conference on computer vision*. Springer, 2012, pp. 746–760.
- [22] A. Dai, A. X. Chang, M. Savva, M. Halber, T. Funkhouser, and M. Nießner, “Scannet: Richly-annotated 3d reconstructions of indoor scenes,” in *Proceedings of the IEEE conference on computer vision and pattern recognition*, 2017, pp. 5828–5839.

- [23] P. Sun, H. Kretzschmar, X. Dotiwalla, A. Chouard, V. Patnaik, P. Tsui, J. Guo, Y. Zhou, Y. Chai, B. Caine, *et al.*, “Scalability in perception for autonomous driving: Waymo open dataset,” in *Proceedings of the IEEE/CVF Conference on Computer Vision and Pattern Recognition*, 2020, pp. 2446–2454.
- [24] A. Gaidon, Q. Wang, Y. Cabon, and E. Vig, “Virtual kitti: An annotated virtual dataset for scene understanding,” in *Proceedings of the IEEE conference on computer vision and pattern recognition workshops*, 2016, pp. 28–37.
- [25] F. Zenke, B. Poole, and S. Ganguli, “Continual learning through synaptic intelligence,” in *International conference on machine learning*. PMLR, 2017, pp. 3987–3995.
- [26] R. Aljundi, F. Babiloni, M. Elhoseiny, M. Rohrbach, and T. Tuytelaars, “Memory aware synapses: Learning what (not) to forget,” in *Proceedings of the European conference on computer vision (ECCV)*, 2018, pp. 139–154.
- [27] A. Chaudhry, P. K. Dokania, T. Ajanthan, and P. H. Torr, “Riemannian walk for incremental learning: Understanding forgetting and intransigence,” in *Proceedings of the European conference on computer vision (ECCV)*, 2018, pp. 532–547.
- [28] G. Hinton, O. Vinyals, and J. Dean, “Distilling the knowledge in a neural network,” *arXiv preprint arXiv:1503.02531*, 2015.
- [29] P. Dhar, R. V. Singh, K.-C. Peng, Z. Wu, and R. Chellappa, “Learning without memorizing,” in *Proceedings of the IEEE/CVF conference on computer vision and pattern recognition*, 2019, pp. 5138–5146.
- [30] A. Rannen, R. Aljundi, M. B. Blaschko, and T. Tuytelaars, “Encoder based lifelong learning,” in *Proceedings of the IEEE international conference on computer vision*, 2017, pp. 1320–1328.
- [31] K. Lee, K. Lee, J. Shin, and H. Lee, “Overcoming catastrophic forgetting with unlabeled data in the wild,” in *Proceedings of the IEEE/CVF International Conference on Computer Vision*, 2019, pp. 312–321.
- [32] A. Douillard, M. Cord, C. Ollion, T. Robert, and E. Valle, “Podnet: Pooled outputs distillation for small-tasks incremental learning,” in *Proceedings of the IEEE/CVF Conference on Computer Vision and Pattern Recognition (CVPR)*, 2020, pp. 1951–1960.
- [33] S. Hou, X. Pan, C. Change Loy, Z. Wang, and D. Lin, “Learning a unified classifier incrementally via rebalancing,” in *Proceedings of the IEEE/CVF Conference on Computer Vision and Pattern Recognition (CVPR)*, 2019, pp. 831–839.
- [34] M. K. Titsias, J. Schwarz, A. G. d. G. Matthews, R. Pascanu, and Y. W. Teh, “Functional regularisation for continual learning with gaussian processes,” *arXiv preprint arXiv:1901.11356*, 2019.
- [35] Y. Pan, F. Li, and W. K. Lee, “Continual deep learning by functional regularisation of memorable past,” *arXiv preprint arXiv:2007.15302*, 2020.
- [36] C. V. Nguyen, Y. Li, T. D. Bui, and R. E. Turner, “Variational continual learning,” in *International Conference on Learning Representations*, 2018.
- [37] A. Chaudhry, M. Rohrbach, M. Elhoseiny, T. Ajanthan, P. K. Dokania, P. H. Torr, and M. Ranzato, “On tiny episodic memories in continual learning,” *arXiv preprint arXiv:1902.10486*, 2019.
- [38] M. Riemer, I. Cases, R. Ajemian, M. Liu, I. Rish, Y. Tu, and G. Tesauro, “Learning to learn without forgetting by maximizing transfer and minimizing interference,” *arXiv preprint arXiv:1810.11910*, 2018.
- [39] J. S. Vitter, “Random sampling with a reservoir,” *ACM Transactions on Mathematical Software (TOMS)*, vol. 11, no. 1, pp. 37–57, 1985.
- [40] D. Lopez-Paz and M. Ranzato, “Gradient episodic memory for continual learning,” *Advances in neural information processing systems*, vol. 30, 2017.
- [41] S.-A. Rebuffi, A. Kolesnikov, G. Sperl, and C. H. Lampert, “icarl: Incremental classifier and representation learning,” in *Proceedings of the IEEE conference on Computer Vision and Pattern Recognition*, 2017, pp. 2001–2010.
- [42] H. Shin, J. K. Lee, J. Kim, and J. Kim, “Continual learning with deep generative replay,” *Advances in neural information processing systems*, vol. 30, 2017.
- [43] M. Riemer, T. Klinger, D. Bouneffouf, and M. Franceschini, “Scalable recollections for continual lifelong learning,” in *Proceedings of the AAAI conference on artificial intelligence*, 2019, pp. 1352–1359.
- [44] M. Rostami, S. Kolouri, and P. K. Pilly, “Complementary learning for overcoming catastrophic forgetting using experience replay,” *arXiv preprint arXiv:1903.04566*, 2019.
- [45] B. Pfülb, A. Gepperth, and B. Bagus, “Continual learning with fully probabilistic models,” *arXiv preprint arXiv:2104.09240*, 2021.
- [46] R. Kemker and C. Kanan, “Fearnnet: Brain-inspired model for incremental learning,” *arXiv preprint arXiv:1711.10563*, 2017.

- [47] S. Gopalakrishnan, P. R. Singh, H. Fayek, S. Ramasamy, and A. Ambikapathi, “Knowledge capture and replay for continual learning,” in *Proceedings of the IEEE/CVF winter conference on applications of computer vision*, 2022, pp. 10–18.
- [48] A. Ayub and A. R. Wagner, “Eec: Learning to encode and regenerate images for continual learning,” *arXiv preprint arXiv:2101.04904*, 2021.
- [49] O. Ostapenko, M. Puscas, T. Klein, P. Jahnichen, and M. Nabi, “Learning to remember: A synaptic plasticity driven framework for continual learning,” in *Proceedings of the IEEE/CVF conference on computer vision and pattern recognition*, 2019, pp. 11 321–11 329.
- [50] Y. X. Wu, L. Herranz, X. Liu, J. van de Weijer, B. Raducanu, and T. Tuytelaars, “Memory replay gans: Learning to generate new categories without forgetting,” in *Proceedings of the 32nd International Conference on Neural Information Processing Systems*, 2018, pp. 5967–5977.
- [51] K. Zhu, W. Zhai, Y. Cao, J. Luo, and Z.-J. Zha, “Self-sustaining representation expansion for non-exemplar class-incremental learning,” in *Proceedings of the IEEE/CVF Conference on Computer Vision and Pattern Recognition*, 2022, pp. 9296–9305.
- [52] X. Liu, C. Wu, M. Menta, L. Herranz, B. Raducanu, A. D. Bagdanov, S. Jui, and J. v. de Weijer, “Generative feature replay for class-incremental learning,” in *Proceedings of the IEEE/CVF Conference on Computer Vision and Pattern Recognition Workshops*, 2020, pp. 226–227.
- [53] A. Iscen, J. Zhang, S. Lazebnik, and C. Schmid, “Memory-efficient incremental learning through feature adaptation,” in *Computer Vision—ECCV 2020: 16th European Conference, Glasgow, UK, August 23–28, 2020, Proceedings, Part XVI 16*. Springer, 2020, pp. 699–715.
- [54] E. Belouadah and A. Popescu, “Il2m: Class incremental learning with dual memory,” in *Proceedings of the IEEE/CVF international conference on computer vision*, 2019, pp. 583–592.
- [55] H. Chawla, A. Varma, E. Arani, and B. Zonooz, “Continual learning of unsupervised monocular depth from videos,” in *Proceedings of the IEEE/CVF Winter Conference on Applications of Computer Vision*, 2024, pp. 8419–8429.
- [56] N. Vödösch, K. Petek, W. Burgard, and A. Valada, “Codeps: Online continual learning for depth estimation and panoptic segmentation,” *arXiv preprint arXiv:2303.10147*, 2023.
- [57] Y. Yang, A. Wong, and S. Soatto, “Dense depth posterior (ddp) from single image and sparse range,” in *Proceedings of the IEEE/CVF Conference on Computer Vision and Pattern Recognition*, 2019, pp. 3353–3362.
- [58] T. Y. Liu, P. Agrawal, A. Chen, B.-W. Hong, and A. Wong, “Monitored distillation for positive congruent depth completion,” in *Computer Vision—ECCV 2022: 17th European Conference, Tel Aviv, Israel, October 23–27, 2022, Proceedings, Part II*. Springer, 2022, pp. 35–53.
- [59] Y. Wu, T. Y. Liu, H. Park, S. Soatto, D. Lao, and A. Wong, “Augundo: Scaling up augmentations for monocular depth completion and estimation,” in *European Conference on Computer Vision*. Springer, 2024.
- [60] H. Park, A. Gupta, and A. Wong, “Test-time adaptation for depth completion,” in *Proceedings of the IEEE/CVF Conference on Computer Vision and Pattern Recognition*, 2024, pp. 20 519–20 529.
- [61] M. Hu, S. Wang, B. Li, S. Ning, L. Fan, and X. Gong, “Penet: Towards precise and efficient image guided depth completion,” in *2021 IEEE International Conference on Robotics and Automation (ICRA)*. IEEE, 2021, pp. 13 656–13 662.
- [62] A. Li, Z. Yuan, Y. Ling, W. Chi, C. Zhang, *et al.*, “A multi-scale guided cascade hourglass network for depth completion,” in *Proceedings of the IEEE/CVF Winter Conference on Applications of Computer Vision*, 2020, pp. 32–40.
- [63] A. Eldesokey, M. Felsberg, K. Holmquist, and M. Persson, “Uncertainty-aware cnns for depth completion: Uncertainty from beginning to end,” in *Proceedings of the IEEE/CVF Conference on Computer Vision and Pattern Recognition (CVPR)*, 2020, pp. 12 014–12 023.
- [64] W. Van Gansbeke, D. Neven, B. De Brabandere, and L. Van Gool, “Sparse and noisy lidar completion with rgb guidance and uncertainty,” in *2019 16th International Conference on Machine Vision Applications (MVA)*. IEEE, 2019, pp. 1–6.
- [65] Y. Zhang and T. Funkhouser, “Deep depth completion of a single rgb-d image,” in *Proceedings of the IEEE Conference on Computer Vision and Pattern Recognition*, 2018, pp. 175–185.
- [66] Y. Zhang, X. Guo, M. Poggi, Z. Zhu, G. Huang, and S. Mattoccia, “Completionformer: Depth completion with convolutions and vision transformers,” in *Proceedings of the IEEE/CVF Conference on Computer Vision and Pattern Recognition*, 2023, pp. 18 527–18 536.
- [67] Z. Yu, Z. Sheng, Z. Zhou, L. Luo, S. Cao, H. Gu, H. Zhang, and H. Shen, “Aggregating feature point cloud for depth completion,” in *Proceedings of the IEEE/CVF International Conference on Computer Vision*, 2023, pp. 8732–8743.

- [68] F. Ma, G. Cavalheiro, and S. Karaman, “Self-supervised sparse-to-dense: Self-supervised depth completion from lidar and monocular camera,” in *2019 International Conference on Robotics and Automation (ICRA)*. IEEE, 2019, pp. 3288–3295.
- [69] S. S. Shivakumar, T. Nguyen, I. D. Miller, S. W. Chen, V. Kumar, and C. J. Taylor, “Dfuset: Deep fusion of rgb and sparse depth information for image guided dense depth completion,” in *2019 IEEE Intelligent Transportation Systems Conference (ITSC)*. IEEE, 2019, pp. 13–20.
- [70] A. Wong, X. Fei, B.-W. Hong, and S. Soatto, “An adaptive framework for learning unsupervised depth completion,” *IEEE Robotics and Automation Letters*, vol. 6, no. 2, pp. 3120–3127, 2021.
- [71] V. Lepetit, F. Moreno-Noguer, and P. Fua, “Epn: An accurate o (n) solution to the pnp problem,” *International journal of computer vision*, vol. 81, no. 2, p. 155, 2009.
- [72] M. A. Fischler and R. C. Bolles, “Random sample consensus: a paradigm for model fitting with applications to image analysis and automated cartography,” *Communications of the ACM*, vol. 24, no. 6, pp. 381–395, 1981.
- [73] A. Lopez-Rodriguez, B. Busam, and K. Mikolajczyk, “Project to adapt: Domain adaptation for depth completion from noisy and sparse sensor data,” in *Proceedings of the Asian Conference on Computer Vision (ACCV)*, 2020.
- [74] J. Jeon, H. Lim, D. U. Seo, and H. Myung, “Struct-mdc: Mesh-refined unsupervised depth completion leveraging structural regularities from visual slam,” in *IEEE Robotics and Automation Letters (RA-L)*, no. 3, 2022, pp. 6391–6398.